

IEEE Copyright Notice

© 2024 IEEE. Personal use of this material is permitted. Permission from IEEE must be obtained for all other uses, in any current or future media, including reprinting/republishing this material for advertising or promotional purposes, creating new collective works, for resale or redistribution to servers or lists, or reuse of any copyrighted component of this work in other works.

arXiv:2406.15538v1 [cs.LG] 21 Jun 2024

Model-Based Generation of Representative Rear-End Crash Scenarios Across the Full Severity Range Using Pre-Crash Data

Jian Wu, Carol Flannagan, Ulrich Sander, and Jonas Bärgrman

Abstract—Generating representative rear-end crash scenarios is crucial for safety assessments of Advanced Driver Assistance Systems (ADAS) and Automated Driving systems (ADS). However, existing methods for scenario generation face challenges such as limited and biased in-depth crash data and difficulties in validation. This study sought to overcome these challenges by combining naturalistic driving data and pre-crash kinematics data from rear-end crashes. The combined dataset was weighted to create a representative dataset of rear-end crash characteristics across the full severity range in the United States. Multivariate distribution models were built for the combined dataset, and a driver behavior model for the following vehicle was created by combining two existing models. Simulations were conducted to generate a set of synthetic rear-end crash scenarios, which were then weighted to create a representative synthetic rear-end crash dataset. Finally, the synthetic dataset was validated by comparing the distributions of parameters and the outcomes (Delta-v, the total change in vehicle velocity over the duration of the crash event) of the generated crashes with those in the original combined dataset. The synthetic crash dataset can be used for the safety assessments of ADAS and ADS and as a benchmark when evaluating the representativeness of scenarios generated through other methods.

Index Terms—Rear-end crash, pre-crash data, crash scenario generation, data combination, virtual safety assessment.

I. INTRODUCTION

ADVANCED Driver Assistance Systems (ADAS) and Automated Driving Systems (ADS) have the potential to improve traffic safety significantly [1]. However, evaluating the safety performance of such systems is still a challenge. Currently, virtual safety assessment is the primary procedure due to its low cost and high efficiency compared to conventional field tests [2]–[5]. Typically, in such a virtual assessment method, a comparison between the ‘baseline’ and ‘treatment’

This work was supported by the FFI program sponsored by Vinnova, the Swedish governmental agency for innovation, as part of the project Improved quantitative driver behavior models and safety assessment methods for ADAS and AD (QUADRI: nr. 2020-05156).

Jian Wu is with the Volvo Cars Safety Center, 41878 Gothenburg, Sweden, and the Department of Mechanics and Maritime Sciences, Chalmers University of Technology, 41756 Gothenburg, Sweden. (e-mail: jian.wu.2@volvocars.com)

Carol Flannagan is with the University of Michigan Transportation Research Institute (UMTRI), Ann Arbor, Michigan 48109, USA, and the Department of Mechanics and Maritime Sciences, Chalmers University, 41756 Gothenburg, Sweden. (email: cacf@umich.edu)

Ulrich Sander is with the Volvo Cars Safety Center, 41878 Gothenburg, Sweden. (e-mail: ulrich.sander@volvocars.com)

Jonas Bärgrman is at the Department of Mechanics and Maritime Sciences, Chalmers University of Technology, 41756 Gothenburg, Sweden. (e-mail: jonas.bargman@chalmers.se)

is conducted to assess a technology. The baseline is a set of scenarios to be analyzed without the technology under assessment, and these scenarios must match the assessment objective and include all relevant elements that may impact the performance of the technology under assessment [6]. A large number of baseline scenarios is essential for making a statistically significant comparison between the baseline and treatment [6]. There are two main approaches to creating a large number of baseline scenarios: traffic-simulation-based [7]–[9] and in-depth-crash-data-based (referred to as IDC-based) [10]–[14].

The traffic-simulation-based approach aims to replicate daily driving activities to generate virtual crashes in a naturalistic driving environment [7]–[9]. Typically, this approach uses road-user behavior models created using naturalistic driving data (NDD) that contain a limited number of crashes, often of minor severity. The simulations are carried out over an extended period, measured in millions of simulated driving hours. Often, it is only the crash avoidance performance of the system that is assessed – by comparing the number of crashes generated through simulations in which the subject vehicle is equipped with the specific ADAS or ADS under assessment to the number of crashes from traffic simulations without the system [15].

The IDC-based approach, on the other hand, uses detailed real-world crash information. This information includes reconstructed or recorded data, such as the pre-crash kinematics of the involved road users. Virtual crashes are generated by sampling from distributions of the parameterized pre-crash kinematics and/or other relevant crash characteristics. The crashes generated serve as the baseline for assessing the safety performance of the ADAS or ADS. Treatment simulations are then executed using the baseline crashes as a starting point but with the ADAS or ADS under assessment included. The outcomes of the baseline and treatment simulations are then compared to assess (for example) the system’s crash avoidance and injury mitigation performance [10]–[14].

Both approaches have their own set of challenges. As noted, the traffic-simulation-based approach takes extensive time to simulate [7]. Also, using NDD as the initial condition for generating crash scenarios may lead to crash characteristics that are significantly different than those in real-world crashes [16]. For example, few higher-severity crashes are typically generated, biasing the assessment towards a baseline/treatment comparison of low-severity crashes (or even to crash surrogates [17]). In addition, crashes generated by the traffic-

simulation-based approach rely heavily on multiple accurate models of road-user behaviors that can produce realistic crashes, representing the real world. However, there is typically a lack of proof of similarity (i.e., validation) between the generated and real-world crashes regarding the characteristics of individual crashes and the characteristics' distributions.

In contrast, the IDC-based approach requires substantial in-depth pre-crash kinematics data. This information is seldom available for most types of scenarios—and when it is, it is typically biased towards severe crashes due to the selection criteria of conventional crash databases. As a result, relying solely on these databases to create synthetic crashes skews the crash generation models, potentially distorting the overall analysis [18]–[20].

This study aims to address these challenges by combining both approaches, creating a dataset of synthetic, passenger-vehicle-involved, rear-end crash scenarios that are representative of the population of such crashes with respect to severity in the United States (referred to as the 'reference dataset' with notation Φ). The dataset is intended for use in the safety assessment of ADAS and ADS and as a benchmark for evaluating the representativeness of scenarios generated through other scenario generation methods.

A synthetic rear-end crash scenario consists of three main components: a speed profile of the lead vehicle, a behavior model of the following vehicle (how it responds to the behavior of the lead vehicle), and the initial states of the scenario. We used the speed profile of the lead vehicle, which is a vehicle kinematics model (instead of a behavior model) because the lead vehicle's behavior is mostly independent of the following vehicle's behavior [21]. The initial states include the speeds of both vehicles and the following distance at the beginning of the scenario.

For the first component, we turned to our previous study [21] in which we modeled the pre-crash lead-vehicle kinematics in rear-end crash scenarios and produced a synthetic dataset of lead-vehicle speed profiles representative of crashes across all severity levels.

The second component, a following-vehicle behavior model, was created by merging two existing driver behavior models [22], [23]. For the third component, data from multiple rear-end crash datasets from various sources were combined and weighted to create a reference dataset of the initial states of rear-end crash scenarios and minimum accelerations of both vehicles. Distributions were then built for this reference dataset.

Once the three components were complete, simulations were conducted to obtain a set of synthetic rear-end crash scenarios. The scenarios were weighted to match the obtained reference datasets, creating a representative synthetic rear-end crash dataset. Finally, this dataset was validated by comparing the parameter distributions of the generated crashes with the reference datasets, as well as by comparing the lead-vehicle Δv (i.e., the total change in vehicle velocity over the duration of the crash event) distributions of the two.

II. DATA

A. Data Sources

The datasets used are from four sources: the Crash Investigation Sampling System (CISS), the Second Strategic Highway Research Program (SHRP2) Naturalistic Driving Study (NDS), the German In-Depth Accident Study (GIDAS) Pre-Crash Matrix (PCM), and our prior study [21].

CISS is a nationally representative sample of crashes in the United States in which at least one light vehicle was towed away from the scene [24], [25]. The data were obtained from comprehensive crash investigations, encompassing examinations of damaged vehicles and crash sites as well as assessments of crash kinematics. CISS includes Event Data Recorder (EDR) data whenever available.

The SHRP2 NDS provides recorded pre-crash information originating from the United States. Over 3,300 passenger vehicles were equipped with a data acquisition system (DAS) to capture four distinct video perspectives, coupled with information extracted from vehicle networks and sensors. Between 2010 and 2013, naturalistic driving data were collected from participants' instrumented vehicles in six locations across the United States. The SHRP2 dataset includes a continuum of conflicts, from near-crashes to (a few) high-severity crashes. The incidents were identified by applying a set of event identification algorithms to the accumulated trip records. In a subsequent manual annotation step, the identified instances were classified by severity level [26].

The GIDAS dataset is a renowned German dataset that comprehensively investigates traffic accidents with personal injury in Germany. The PCM subset of the GIDAS dataset contains reconstructed pre-crash time-series data that describes the pre-crash trajectories and provides digitized information about the road layout and potential sight obstructions. Since its inception in 2011, the PCM dataset has provided time-series data of the phases leading up to a diverse array of crash scenarios, encompassing a temporal span of up to five seconds before the events [27]. Note, however, that the reconstructions of the pre-crash phase are based on evidence from the accident site and eyewitnesses; detailed driver behavior is unknown.

Among the three datasets, the SHRP2 dataset (with a frequency of 10 Hz) covers incidents from near-crashes to severe crashes, while the GIDAS-PCM dataset (with a frequency of 100 Hz) only includes crashes resulting in personal injury, and the CISS dataset (with a frequency varying from 1 to 10 Hz) only contains accidents involving towed vehicles. Consequently, the latter two datasets exclude low-severity crashes, and the censoring boundary is not obvious to quantify.

B. Datasets

Table I shows the datasets used in this study. Seven datasets derived from the four sources were used as input. Four intermediate datasets were created from these to obtain three output datasets. Datasets other than those used as input are introduced later (in Section III). Each dataset is named according to the source type, with a postfix indicating the kind of information included. (See Table I for details).

TABLE I
DATASETS IN THE STUDY

Type	Notation*	Source	Description	Signals	Sample size
Input	CISS_m	CISS	General rear-end crash data	m_f, m_l	748
	CISS_f	CISS	Rear-end pre-crash data (SV-striking)	$v_f, \Delta v_l$	408
	SHRP2_f	SHRP2	Rear-end pre-crash data (SV-striking)	$v_f, \Delta v_f$	116
	SHRP2_b	SHRP2	Further annotated rear-end pre-crash data	$v_f, v_l, d, \Delta v_f$	37
	PCM_b	GIDAS-PCM	Reconstructed rear-end crash data	$v_f, v_l, d, \Delta v_l$	861
	REF_l	Previous study	Combined rear-end crash lead-vehicle speed profile	$v_c, a_1, a_2, \tau_s, \tau_1, \tau_2, \Delta v_l$	132
	REF_sl	Previous study	Synthetic lead-vehicle speed profiles	$v_c, a_1, a_2, \tau_s, \tau_1, \tau_2$	10,000
Intermediate	COM_f	-	Combined following-vehicle-information dataset	-	524
	COM_b	-	Combined both-vehicle-information dataset	-	913
	REF_f	-	Reference following-vehicle-information dataset	-	324
	REF_i	-	Reference intermediate dataset	-	10,000
Output	REF_b	-	General rear-end crash data	-	852
	REF_sb	-	Synthetic both-vehicle-information dataset	-	10,000
	REF_ss	-	Synthetic rear-end crash dataset	-	5,000

* Each dataset is named according to the source type (i.e., REF: reference, COM: combined), with a postfix indicating the type of information that the dataset includes (m: mass information, l: lead-vehicle information, f: following-vehicle information, b: both-vehicle information, i: intermediate, sl: synthetic lead-vehicle information, sb: synthetic both-vehicle information, and ss: synthetic crash scenario).

CISS_m (n = 748) includes all CISS rear-end crash records, which contain the curb weight of the lead and following vehicle, m_f and m_l (kg). CISS_f (n = 408) comprises EDR-based pre-crash data from CISS rear-end crashes in which the subject vehicle (SV) was the striking/following vehicle. Signals extracted from the CISS_f dataset were the following-vehicle speed v_f (m/s) and Delta-v of the lead vehicle Δv_l (m/s). SHRP2_f (n = 116) consists of SHRP2 rear-end pre-crash events recorded by the striking vehicles. The signal v_f and its derivative signal, the following vehicle's Delta-v Δv_f (m/s), were the signals used in the dataset. SHRP2_b (n = 37) was generated by further annotating a subset of the SHRP2 rear-end crashes included in SHRP2_f. For each crash, the following distance d (m) was estimated by Victor et al. [28] using image processing, and the lead-vehicle speed v_l (m/s) was deduced based on v_f and d . PCM_b (n = 861) contains reconstructed rear-end crash data from the GIDAS-PCM dataset, including $v_f, v_l, d,$ and Δv_l signals. (Note that we excluded one pedal misapplication case in which the driver of the following vehicle accidentally pushed the acceleration pedal when approaching the lead vehicle.)

In our previous study [21], we fitted the lead-vehicle speed profiles five seconds before the impact in recorded rear-end crashes from the SHRP2 and CISS datasets into a piecewise linear model. This model simplifies a speed profile as a sequence of, at most, three straight lines; the slopes of the lines are the fitted accelerations. (Note that there can be cases with fewer than three segments.) Each lead-vehicle speed profile was parameterized as a six-dimensional vector: $[v_c, a_1, a_2, \tau_s, \tau_1, \tau_2]$. Fig. 1 shows an example with three segments (going backward in time from time zero, the impact moment):

- Segment S: The lead vehicle maintains a steady speed in this segment. τ_s is the segment duration, and v_c is the lead vehicle's estimated speed at time zero.
- Segment 1: The lead vehicle keeps a non-zero constant acceleration in this segment. τ_1 is the segment duration, and a_1 is the fitted constant acceleration.
- Segment 2: The lead vehicle keeps a constant acceleration

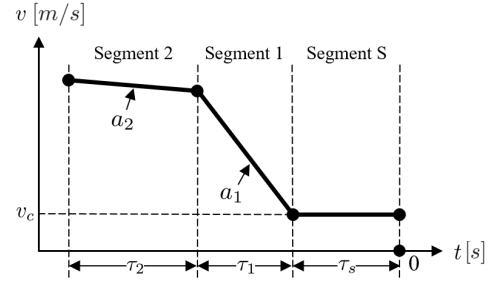


Fig. 1. Three selected segments of the lead-vehicle speed profile in a rear-end crash.

in this segment. τ_2 is the segment duration, and a_2 is the fitted constant acceleration.

This piecewise linear model will be reintroduced in Section III-C.

REF_l and REF_sl were also derived from our previous study [21]. REF_l (n = 132) contains 132 rear-end crash lead-vehicle speed profiles, of which 83 and 49 come from the SHRP2 and CISS datasets, respectively. The samples in the dataset were weighted to create a reference dataset of the lead-vehicle kinematics covering the full range of crash severity (from non-severe to severe). In this study, the lead vehicle's Delta-v (Δv_l) was obtained by either extracting the signal (for CISS crashes) or estimating it as the difference between the post- and pre-impact lead-vehicle speed (for SHRP2 crashes). REF_sl (n = 10,000) is a dataset of 10,000 synthetic lead-vehicle speed profiles generated by the distribution models built on REF_l. The two datasets can be considered reference datasets of lead-vehicle kinematics in rear-end crashes.

C. Event Data Extraction

CISS pre-crash data typically include five seconds before the impact, while SHRP2 and GIDAS-PCM data cover a longer duration. The start time of all events was thus set to five seconds before the impact (defined as time zero) to make all events equivalent.

For each crash event in CISS_f, only the following vehicle's initial speed (i.e., the speed at $t = -5$ s) was extracted.

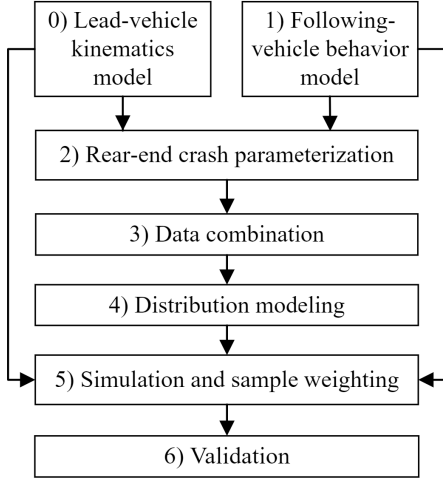


Fig. 2. Flowchart of the methodology. Step 0 (the lead-vehicle kinematics model) was performed in our previous study [21].

In contrast, we extracted the whole events (all the time-series data) for SHRP2- and GIDAS-PCM-sourced datasets. As in the previous study [21], the extracted event duration for datasets SHRP2_f, SHRP2_b, and PCM_b spanned from -5 to -0.3 s, ending just before impact to avoid a possible sharp acceleration pulse.

III. METHODOLOGY

In this study, the following six steps were performed in order:

- 1) Following-vehicle behavior model creation
- 2) Rear-end crash parameterization
- 3) Data combination
- 4) Distribution modeling
- 5) Simulation and sample weighting
- 6) Validation

Fig. 2 shows how these steps are interconnected. Step 0 (the lead-vehicle kinematics model) was performed in our previous study [21]. Steps 0 and 1 (the following-vehicle behavior model) provided the basis for Step 2, which simplified a rear-end crash event by representing it as a set of parameters. Then, Step 3 created a reference dataset of a subset of parameters (initial states of rear-end crash scenarios and minimum accelerations of both vehicles), and Step 4 built a distribution model on the reference dataset. The simulation and sample weighting step (Step 5) was carried out using the distribution model and the following-vehicle behavior model, as well as the lead-vehicle kinematics model from the previous study [21]. The step resulted in the synthetic rear-end crash dataset. Finally, we validated the synthetic dataset in Step 6.

A. Step 1: Following-vehicle Behavior Model Creation

The following-vehicle behavior model is a combination of two existing driver behavior models: 1) the modified intelligent driver model [22], which describes the longitudinal vehicle control behavior during car following, and 2) the driver

pre-crash brake response model [23], which predicts when and how the driver brakes in the rear-end pre-crash phase. Additionally, the model includes the possibility of generating abnormal driver acceleration behavior under some conditions, which is introduced later in this sub-section.

1) *Modified intelligent driver model*: The modified intelligent driver model is a modification of the Intelligent Driver Model (IDM), a time-continuous car-following model frequently used in traffic flow modeling. In this model, only longitudinal movement is considered. The acceleration of vehicle α , a_α (m/s^2), is computed as

$$a_\alpha = a \cdot \left[1 - \left(\frac{v_\alpha}{v_0} \right)^4 - \left(\frac{d_\alpha^*}{d_\alpha} \right)^2 \right], \quad (1)$$

where v_α (m/s) is the speed of vehicle α , a (m/s^2) is the maximum acceleration, v_0 (m/s) is the desired speed of vehicle α in free traffic, d_α (m) is the following distance, and d_α^* (m) is the desired minimum following distance, which is defined as

$$d_\alpha^* = d^*(v_\alpha, \Delta v_\alpha) = d_0 + v_\alpha T + c \frac{v_\alpha^2}{b} - \frac{v_\alpha \Delta v_\alpha}{2\sqrt{ab}}, \quad (2)$$

where Δv_α (m/s) is the relative speed of the lead vehicle of vehicle α , d_0 (m) is the jam distance, T (s) is the minimum time headway to the vehicle in front, b (m/s^2) is the comfortable braking deceleration, and c is the coefficient added in the modified model to increase the desired minimum following distance. v_0 was set as the road speed limit. As suggested by Derbel et al. [22], in this work a , b , and c were set to 3 m/s^2 , 4 m/s^2 , and 0.4 , respectively, and $T \sim \mathcal{N}(1.5, 0.16)$ s.

2) *Driver pre-crash brake response model*: This model, proposed by Svärd et al. [23], [29] (denoted as model BWL_{rc} in their paper), is a driver model that quantitatively predicts how and when the driver will initiate and modulate the pre-crash brake response. The model uses the accumulation of the prediction error of looming (the relative expansion rate of the lead vehicle's image on the retina of the following vehicle [30]) as the basis for the driver's braking response. In addition, the model considers the driver's off-road glance behavior. Specifically, the model applies an off-road glance looming weight parameter to account for the driver's partial perception of looming during off-road glances. The driver's brake responses can thus occur quickly since the driver accumulates evidence even when not looking directly at the road. The model parameters in this study were set the same as the fitting results calibrated for the 13 SHRP2 rear-end pre-crash events [23]. The model's inputs are looming, the glance off-road signal, and the minimum acceleration (or maximum deceleration) of the following vehicle $a_{f,min}$ (m/s^2). The model outputs a non-positive acceleration a_b (m/s^2).

Research [28], [31], [32] has shown that the role of distraction in rear-end crashes is influenced by situational urgency. This influence is operationalized by emphasizing off-road glances after the time to collision (TTC) falls below a certain threshold instead of focusing on off-road glances throughout the event. Therefore, to describe the glance-off-road behavior of the following vehicle's driver, we used the

parameter suggested in the reference study [31]: the glance off-road overshoot t_g (s) after $TTC^{-1} = 0.2 \text{ s}^{-1}$. The overshoot is the off-road glance that occurs after $TTC^{-1} = 0.2 \text{ s}^{-1}$ (hereafter called the *anchor point*) and continues for a duration of t_g seconds. TTC^{-1} is the inverse time to collision (s^{-1}). The same process in the reference study was followed to create the reference distribution for t_g , using glance behavior for normal driving from the SHRP2 dataset.

3) *Abnormal acceleration behavior*: In the PCM_b dataset, there are crashes in which both the lead and following vehicles were initially stationary. Then, after a while, the following vehicle started accelerating until it hit the lead vehicle. Unlike the excluded case of pedal misapplication, the driver of the following vehicle seemed to ignore the lead vehicle completely in these cases, possibly due to distraction.

Two parameters, a_a and t_a , were added to the following-vehicle behavior model to account for these 'abnormal' acceleration behaviors. When the behaviors occurred, the following vehicle was assumed to keep a constant acceleration a_a , which was set to 1.8 m/s^2 (the mean of the acceleration values in the abnormal acceleration cases in the PCM_b dataset). t_a is the time duration from the event's start ($t = -5 \text{ s}$) to the beginning of the abnormal behavior of the following vehicle's driver (s). If t_a is equal to or greater than five seconds, then no abnormal acceleration behavior is present (i.e., the following vehicle does not have time to initiate acceleration before the crash). However, if t_a is less than five seconds, then the lead vehicle will not be taken into account (i.e., the model will act as if there is no lead vehicle) in the calculation of $a_{i,a}$ after t_a from the event's start (i.e., $t = t_a - 5$). The reference distribution of t_a was obtained by fitting the data of t_a in cases with abnormal acceleration behaviors into a normal distribution (see Section IV-B1 for further information regarding the fitting process).

4) *Combined following-vehicle behavior model*: We combined the modified IDM, the driver pre-crash brake response model, and the two abnormal acceleration behavior parameters to create a combined following-vehicle behavior model (referred to as 'the following-vehicle behavior model'). In the combined model, when abnormal acceleration behavior occurs, the output acceleration is the acceleration of the modified IDM, ignoring the lead vehicle. Otherwise, the modified IDM only describes the driver's acceleration behavior, and the brake response model describes the braking behavior. Hence, the acceleration of vehicle i (a_i , m/s^2) is computed as

$$a_i = \begin{cases} 0, & \text{if } t < t_a - 5 < 0 \\ a_a, & \text{if } t_a < 5 \text{ \& } t > t_a - 5 \\ \max(a_{i,a}, 0), & \text{if } a_{i,b} = 0 \text{ \& } t_a \geq 5 \\ a_{i,b}, & \text{otherwise.} \end{cases}, \quad (3)$$

where $a_{i,b}$ is the output acceleration of the driver pre-crash brake response model, $a_{i,a}$ is the output acceleration of the modified IDM, and a_a is the constant acceleration of the following vehicle when the abnormal acceleration behavior occurs. In summary, four parameters are used in the following-vehicle behavior model: $a_{f,min}$, t_g , T , and t_a .

B. Step 2: Rear-end Crash Parameterization

In this step, we parameterized a rear-end crash as a twelve-dimensional vector which considers the initial states of rear-end crash scenarios, the following-vehicle behavior model, and the parameterized lead-vehicle speed profile (see Table II). The parameters can be divided into three types: 1) both-vehicle-related (d_{init}), 2) following-vehicle-related ($v_{f,init}$, $a_{f,min}$, T , t_g , t_a), and 3) lead-vehicle-related ($v_{l,init}$, a_1 , a_2 , τ_s , τ_1 , τ_2). The rationale is that, for instance, $a_{f,min}$ and t_g affect the following vehicle's braking behavior, while T and t_a affect the following vehicle's acceleration behavior.

C. Step 3: Data Combination

It would be ideal to create a reference dataset for the parameterized rear-end crashes directly from a single source of crash data. However, none of the available datasets alone could serve as a reference dataset since they all have limitations. For instance, only SHRP2_b and PCM_b contain information about both vehicles, allowing for joint distribution of the twelve parameters. The other datasets either contain information about only one vehicle's pre-crash dynamics (e.g., SHRP2_f) or general crash data without detailed vehicle dynamics (CISS_m). SHRP2_b, for example, has a relatively small sample size, and the quality of the lead-vehicle speed signal in the dataset is limited since it was deduced by the following distance, which was estimated using image processing on relatively low-quality video. Further, as previously mentioned, PCM_b is biased towards severe crashes. Also, in the reconstruction process for the cases in PCM_b, it is usually assumed that the lead vehicle was moving with constant acceleration or deceleration before the crash when the evidence for a detailed speed profile is lacking. However, our previous study [21] has shown that lead-vehicle speed profiles can take more forms in the pre-crash phase. Since both SHRP2_b and PCM_b lack a high-quality lead-vehicle speed signal, the initial speed and minimum acceleration of the lead vehicle ($v_{l,init}$ and $a_{l,min}$) were selected to represent the lead-vehicle kinematics for the two datasets.

Consequently, it is not feasible to create a reference dataset of all twelve parameters directly from the available datasets. We then created several reference datasets of subsets of parameters as an intermediate step in building the final reference database. As mentioned in Section I, a synthetic rear-end crash scenario consists of three main components: the lead-vehicle speed profile, the following-vehicle behavior model, and the initial states of the scenario. The synthetic lead-vehicle speed profile dataset (REF_sl) from our previous study [21] serves as a reference dataset of lead-vehicle-related parameters. Therefore, the challenge is to create another reference dataset containing the remaining parameters, which can be linked to REF_sl so that we can combine them to create synthetic crash scenarios. The final dataset, REF_b, is a reference dataset of the initial states of the crash scenarios and minimum accelerations of both vehicles: $\tilde{\Phi}(d_{init}, v_{f,init}, a_{f,min}, v_{l,init}, a_{l,min})$. The parameters d_{init} , $v_{f,init}$, and $v_{l,init}$ are used for setting the initial states of the overall scenario; $a_{f,min}$ is required for

TABLE II
DEFINITIONS OF THE TWELVE PARAMETERS

Parameter	Definition	Unit	Type
d_{init}	Following distance at the initial*	m	Both-vehicle-related
$v_{f,init}$	Following vehicle's speed at the initial	m/s	Following-vehicle-related
$a_{f,min}$	Minimum fitted following-vehicle acceleration	m/s ²	Following-vehicle-related
T	Minimum time headway to the lead vehicle	s	Following-vehicle related
t_g	Glance off-road overshoot of the following vehicle's driver	s	Following-vehicle-related
t_a	Duration from the event's start to the beginning of the abnormal behavior of the following vehicle's driver	s	Following-vehicle-related
$v_{l,init}$ **	Lead vehicle's speed at the initial	m/s	Lead-vehicle-related
a_1	Fitted acceleration of Segment 1 of the lead-vehicle speed profile	m/s ²	Lead-vehicle-related
a_2	Fitted acceleration of Segment 2 of the lead-vehicle speed profile	m/s ²	Lead-vehicle-related
τ_s	Duration of Segment S of the lead-vehicle speed profile	s	Lead-vehicle-related
τ_1	Duration of Segment 1 of the lead-vehicle speed profile	s	Lead-vehicle-related
τ_2	Duration of Segment 2 of the lead-vehicle speed profile	s	Lead-vehicle-related

* The initial moment refers to $t = -5$ s for extracted crash events.

** $v_{l,init} = v_c - a_1 \tau_1 - a_2 \tau_2$.

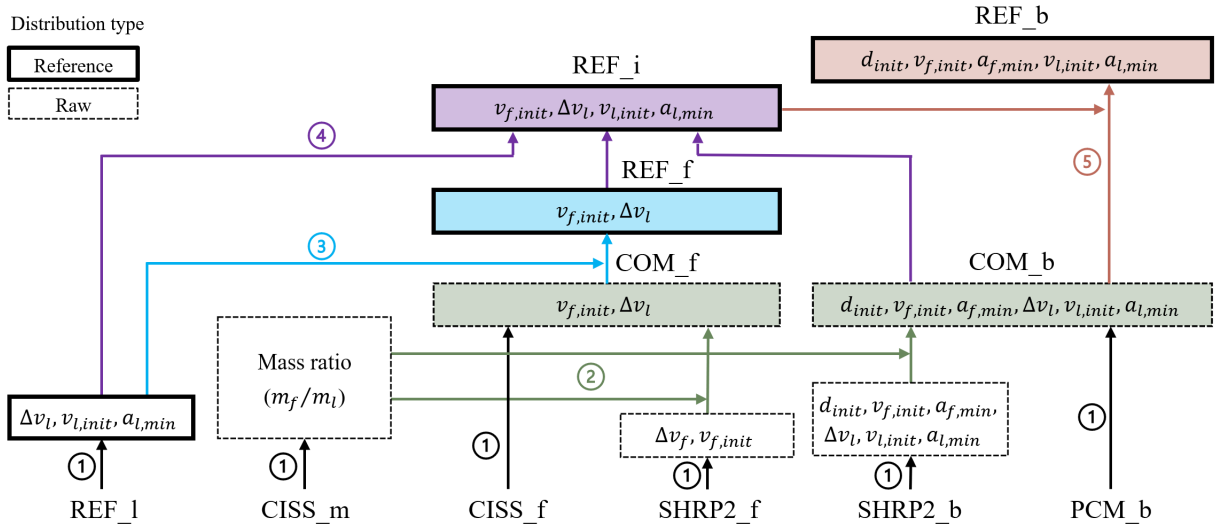


Fig. 3. Flowchart of the data combination. Reference and raw datasets are marked by solid and dashed lines, respectively. Colored arrows and numbers indicate sub-steps. The outcome is the dataset REF_b, the reference dataset of d_{init} , $v_{f,init}$, $a_{f,min}$, $v_{l,init}$, and $a_{l,min}$.

the following-vehicle model. The parameters $v_{l,init}$ and $a_{l,min}$ are common to both REF_b and REF_sl, so they can be used to link any data point in the distribution to a set of synthetic lead-vehicle speed profiles in REF_sl.

Fig. 3 shows the data combination process applied to obtain REF_b; the five sub-steps are numbered and color-coded. Sub-step 1 extracts relevant signals from each dataset. Sub-step 2 deduces the Delta-v of the lead vehicle and combines the following-vehicle-related and both-vehicle-related datasets, respectively. To finally obtain REF_b, sub-steps 3-5 apply sample weight adjustments to reduce biases in the datasets.

Sub-step 1 (Extract signals): Relevant signals from each dataset were extracted: specifically, the speed profiles of the lead and following vehicles in SHRP2_b and PCM_b were fitted into the six-parameter piecewise linear model and simplified as (at most) three consecutive straight lines (see Fig. 1). The minimum fitted acceleration for all segments was also extracted for each speed profile. Finally, the following parameters were extracted for each crash event in SHRP2_b and PCM_b: d_{init} , $v_{f,init}$, $a_{f,min}$, $v_{l,init}$, and $a_{l,min}$. The

lead vehicle's minimum fitted acceleration ($a_{l,min}$) was also extracted in REF_1.

Sub-step 2 (Deduce Delta-v): Δv_l is used as the indicator of crash severity. REF_1 contains the reference distribution of Δv_l , $\tilde{\Phi}(\Delta v_l)$, which was further used to mitigate the severity level bias in other raw datasets (such as CISS_f and SHRP2_f) in later sub-steps. However, SHRP2_f and SHRP2_b can only provide Delta-v of the following vehicle, Δv_f . Therefore, in this sub-step, the mass ratio (m_f/m_l) data extracted from CISS_m was fitted into a generalized gamma distribution, which was then used to transform the Δv_f signal in the two datasets (SHRP2_f and SHRP2_b) to Δv_l based on conservation of momentum:

$$\Delta v_l = -\frac{m_f}{m_l} \Delta v_f. \quad (4)$$

After obtaining Δv_l for SHRP2_f and SHRP2_b, we combined CISS_f and SHRP2_f into one dataset (referred to as COM_f). We also combined SHRP2_b and PCM_b into another dataset (COM_b).

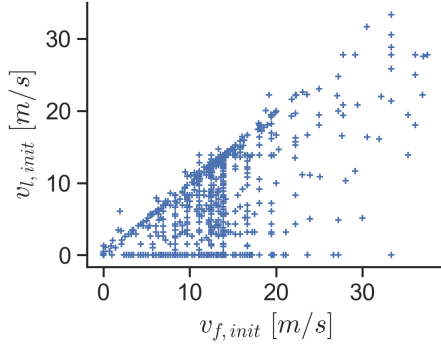


Fig. 4. Scatter plot of $v_{f,init}$ and $v_{l,init}$ for COM_b. In most cases, $v_{l,init}$ is no larger than $v_{f,init}$.

Sub-step 3 (Obtain REF_f): The dataset COM_f is biased towards severe crashes because some of the data come from CISS. Thus, this sub-step developed case weights that adjust the COM_f representation to match the reference distribution of Δv_l from REF_1 using the *k-nearest neighbors (KNN) sample weighting method* to assign weights to the samples in COM_f. (See Appendix A for further information regarding this method.) The new weighted dataset is called REF_f.

Sub-step 4 (Obtain REF_i): This sub-step created an intermediate reference dataset (REF_i, as shown in Fig. 3) with as many parameters as possible, which was used for weighting COM_b to reduce bias in those parameters. REF_i was created by combining two reference datasets: REF_f, obtained in the previous sub-step, and the reference dataset of lead-vehicle kinematics (REF_1). The resulting dataset contains the Delta-v and minimum fitted acceleration of the lead vehicle, as well as the initial speeds of both vehicles (Δv_l , $a_{l,min}$, $v_{f,init}$, and $v_{l,init}$).

To obtain REF_i, we randomly selected (with replacement) an equal number of samples from both reference datasets (REF_f and REF_1). Then, we employed a *pairing algorithm* to pair the selected samples from the two datasets one by one so that the pairs would preserve the correlation structure among the parameters (Δv_l , $a_{l,min}$, $v_{f,init}$, and $v_{l,init}$).

To design the pairing algorithm, we first investigated the correlation structure among the parameters. We computed the correlations among the three parameters in REF_1: the lead vehicle’s Delta-v, initial speed, and minimum fitted acceleration (Δv_l , $v_{l,init}$, and $a_{l,min}$). The results show that the initial speed of the lead vehicle ($v_{l,init}$) is highly correlated with the minimum fitted acceleration of the lead vehicle ($a_{l,min}$). However, Δv_l is only weakly correlated with the other two parameters. (A Pearson correlation coefficient [33] with an absolute value smaller than 0.3 indicates a weak correlation; see Section IV for further information regarding the correlation assessment.) In this study, for the sake of simplicity, we ignored the weak correlation and considered Δv_l to be independent of the other two parameters ($v_{l,init}$ and $a_{l,min}$). Since REF_f also contains Δv_l , we can simply sample $v_{l,init}$ and $a_{l,min}$ (instead of all three parameters) from REF_1. Then, the pairing algorithm must pair those

samples of the two parameters with samples from REF_f (i.e., the reference dataset of the following vehicle’s initial speed and Delta-v of the lead vehicle), in order to preserve the correlation structure among those parameters. Since the samples were randomly drawn from the two reference datasets, the correlations between parameters sampled jointly within each dataset (i.e., the correlations between $v_{f,init}$ and Δv_l and between $v_{l,init}$ and $a_{l,min}$) should be preserved naturally. Therefore, we only need a pairing process to preserve the correlations between $v_{f,init}$ and $v_{l,init}$ and between $v_{f,init}$ and $a_{l,min}$.

The pairing process starts with computing the correlation values. Since no reference dataset containing $v_{f,init}$, $v_{l,init}$, and $a_{l,min}$ was available, we gathered information on both vehicles from the COM_b dataset, the only dataset that contains the three parameters and Δv_l . However, we observed that COM_b has substantial biases in the Delta-v of the lead vehicle (Δv_l) and the initial speed of the following vehicle ($v_{f,init}$). For Δv_l , the bias is inherited as COM_b contains the dataset PCM_b. For $v_{f,init}$, 15% of the cases in COM_b (mostly cases from PCM_b) have a $v_{f,init}$ of exactly 50 km/h. This may be because the following vehicle was assumed to be driven at the speed limit (i.e., 50 km/h) during the reconstruction, as no detailed information was available. To mitigate the biases in these two parameters, the samples in COM_b were weighted using the KNN sample weighting method to match REF_f. We then used the “weights” package in R [34] to compute the two (Pearson) correlation coefficients for the weighted data: $\tilde{r}(v_{f,init}, v_{l,init}) = 0.78$ and $\tilde{r}(v_{f,init}, a_{l,min}) = -0.54$. (Note that, before weighting, those two correlations were 0.53 and -0.20, respectively.) In addition to the strong correlation between the initial speeds of both vehicles, we observed that $v_{l,init}$ is no larger than $v_{f,init}$ in most cases, as shown in Fig. 4.

Based on these observations, Algorithm 2 was developed to pair samples from two datasets, preserving the two correlations, and ensuring that $v_{l,init}$ is no larger than $v_{f,init}$ in most cases. (Algorithm 2 is described in detail in Appendix B.) The pairing results (i.e., REF_i) were used as an approximation for the reference dataset of the four parameters ($\Phi(v_{f,init}, \Delta v_l, v_{l,init}, a_{l,min})$).

Sub-step 5 (Obtain REF_b): At this point REF_i and COM_b were in place, so we created the target dataset REF_b, the reference dataset of the initial states and the two minimum fitted accelerations (d_{init} , $v_{f,init}$, $a_{f,min}$, $v_{l,init}$, and $a_{l,min}$). Again, we weighted samples in COM_b with the KNN sample weighting method to match REF_i, in order to mitigate biases in the four parameters ($v_{f,init}$, Δv_l , $v_{l,init}$, and $a_{l,min}$).

D. Step 4: Distribution Modeling

This step constructed a comprehensive distribution model for REF_b and used the model to generate a synthetic dataset, which is used in the next step to generate representative rear-end crashes.

Because of the large number of parameters and the complexity of the distribution, REF_b was divided into six sub-datasets (referred to as S1-6) that were modeled separately,

using the multivariate distribution modeling method proposed in our previous study [21]. The six sub-datasets were categorized based on the relationship between the initial speeds of both vehicles, whether the following vehicle braked, and whether any vehicle was initially at a standstill (see Section IV for further information). The overall distribution model for REF_b, which can be seen as a mixture distribution model, was derived by combining the distribution models for all sub-datasets according to their relative proportions in REF_b. A synthetic dataset containing synthetic both-vehicle information (referred to as REF_sb) with a sample size of 10,000 was then built with samples generated from the overall distribution model.

E. Step 5: Simulation and Sample Weighting

This step created a set of synthetic rear-end crashes representative of the population of such crashes with respect to severity based on REF_sl, REF_sb, and the reference marginal distributions for the three parameters T , t_g , and t_a (obtained in the previous steps). We first ran simulations of rear-end conflicts under different kinematic parameter settings drawn from the distribution(s) developed in the previous steps. Second, we selected valid simulations (defined in the following subsection) from the simulated set. Finally, the selected crashes were weighted using Iterative proportional fitting (IPF) [35] so that the marginal distributions of parameters for the selected crashes matched the reference distributions. We describe these three sub-steps (simulation setup, generation of synthetic rear-end crashes, and creation of a representative set of synthetic rear-end crashes) in more detail below.

1) *Simulation setup*: The simulation frequency is 20 Hz, and t_{sim} is the simulation time (s). At the start of each simulation ($t_{sim} = 0$ s), the initial states are set according to these three parameters: the initial following distance and the initial speeds of both vehicles (d_{init} , $v_{f,init}$, and $v_{l,init}$). The lead vehicle follows its synthetic speed profile (the six-parameter model; $[v_{l,init}, a_1, a_2, \tau_s, \tau_1, \tau_2]$) until the simulation time reaches five seconds ($t_{sim} = 5$ s), after which it will keep its speed constant. Meanwhile, the following vehicle follows the acceleration computed by the following-vehicle behavior model (see Section III-A). The simulation stops if a crash happens or a maximum simulation time is reached.

To be consistent with the input data of this study, a *valid simulation* must fulfill two conditions: 1) a crash happens and 2) the crash moment t_c is approximately five seconds after the start of the simulation (as the five seconds pre-crash data were extracted for all crashes in the original datasets). That is, as noted earlier, not all simulations met the conditions; some produced crashes that did not belong to the final dataset. However, it is unnecessarily stringent to have the crash occur exactly five seconds after starting the simulation. To provide some margin for the crash timing, a crash moment error t_e ($= t_c - 5$) was created. The second condition then becomes $|t_e| \leq t_{e,thd}$, where $t_{e,thd}$ is a predefined threshold value, set to 0.2 s in this work. (See Section IV for further information regarding the choice of $t_{e,thd}$.) In addition, the maximum simulation time was set to six seconds.

2) *Generation of synthetic rear-end crashes*: This sub-step ran simulations and searched for the valid ones, in order to create a set of synthetic rear-end crashes. A matching algorithm was used to (first) create combinations of parameters among REF_sl and REF_sb (the synthetic datasets of lead-vehicle speed profiles, initial states, and minimum fitted accelerations) and marginal distributions of the three parameters (T , t_g , and t_a) for simulation and (second) to search for valid simulations (defined in the previous sub-step). REF_sl contains seven parameters: $v_{l,init}$, $a_{l,min}$, a_1 , a_2 , τ_s , τ_1 , and τ_2 . The parameter $a_{l,min}$ was computed for REF_sl the same way it was for REF_l. REF_sb contains five parameters: d_{init} , $v_{f,init}$, $a_{f,min}$, $v_{l,init}$, and $a_{l,min}$. Because $v_{l,init}$ and $a_{l,min}$ are common to both, they were used to link samples from the two datasets. We could not simulate all potential parameter combinations due to the high computational load. Therefore, for each sample drawn from REF_sb, a *matching algorithm* was designed to stop looping after obtaining a valid simulation or reaching a predefined maximum number of iterations. The algorithm is briefly described below (with further information in Appendix C).

- 1) Draw N samples, with replacement, from REF_sl and REF_sb: $U = \{\mathbf{U}_i \mid i \in [1, N]\}$ and $V = \{\mathbf{V}_j \mid j \in [1, N]\}$.
- 2) For $j = 1$ to N :
 - a) Compute the Euclidean distance (based on the common parameters $v_{l,init}$ and $a_{l,min}$) between \mathbf{V}_j and each sample in set U , select the samples with a Euclidean distance no larger than a predefined threshold $d_{e,thd}$ as the pairing candidates of \mathbf{V}_j , and save the samples as set W .
 - b) Update set W according to the sub-dataset which \mathbf{V}_j belongs to. For instance, a \mathbf{V}_j from sub-dataset 1 (S1) requires that $v_{f,init} > v_{l,init} > 0$.
 - c) Create sets of candidates for the three parameters T , t_g , and t_a : \bar{T}^* , \bar{t}_g^* , and \bar{t}_a^* . Note that, in those sets, the samples are ordered randomly.
 - d) Loop through W , \bar{T}^* , \bar{t}_g^* , and \bar{t}_a^* until a valid simulation is obtained or the predefined maximum number of iterations is reached. Save the log when there is a valid simulation.

3) *Creation of a representative set of synthetic rear-end crashes*: A synthetic rear-end crash dataset (REF_ss) was created, which includes all valid simulations. The next step was weighting samples in the synthetic dataset to match the two reference datasets (REF_sl and REF_sb) and the reference marginal distributions of the remaining three parameters (T , t_g , and t_a) in the following-vehicle behavior model. It is important to note that when modeling the two reference datasets, each one was split into multiple sub-datasets so that simpler models could be used for each sub-dataset. The overall distribution model was then derived by combining the distribution models for the sub-datasets according to the sub-dataset proportions.

The objectives of this sample weighting were to retain 1) the reference marginal distribution of each of the three parameters (T , t_g , and t_a), 2) the proportion of each sub-dataset, and

3) the marginal distribution of each parameter for each sub-dataset instead of the whole. Iterative proportional fitting (IPF) [35] was used to achieve these objectives. In the algorithm, the Kolmogorov–Smirnov (KS) statistic was used to measure the difference between each weighted marginal distribution and its corresponding reference distribution. The implementation consisted of the following steps:

- 1) Set initial weight for all samples to 1: $w_i^{(0)} = 1, \forall i \in [1, N]$.
- 2) For iteration number $k = 1$ to 100:
 - a) For each parameter other than the three parameters (T , t_g , and t_a) of each sub-dataset, update the weights for samples in the sub-dataset using IPF.
 - b) For each of the three parameters (T , t_g , and t_a), update the weights for all samples using IPF.
 - c) Scale the weights so that $\sum_{i=1}^N w_i^{(k)} = N$.
 - d) Compute the KS statistic between the weighted synthetic crash dataset and corresponding reference distributions with the weighted two-sample KS tests using the "Ecume" package in R [36]: $\{s_j^{(k)} | \forall j \in [1, n]\}$.
 - i) For each sub-dataset, compute the KS statistic between the marginal distribution in the sub-dataset and the reference distribution for each parameter other than the three parameters (T , t_g , and t_a).
 - ii) For each of the three parameters (T , t_g , and t_a), compute the KS statistic between the weighted marginal distribution in the overall synthetic crash dataset and the reference dataset.
 - e) Compute the loss: $L_w^{(k)} = \sum_{j=1}^n [(s_j^{(k)})^2 \sum w_{l_j}^{(k)}]$, where $w_{l_j}^{(k)}$ is the weight for the corresponding sample of $s_j^{(k)}$.
- 3) Select the optimal weights with the minimum loss: $\{w_i^{(k^*)} | i \in [1, N]\}$, where $k^* = \arg \min_k (\{L_w^{(k)} | k \in [1, n]\})$.

F. Step 6: Validation

In terms of validation, firstly, all three objectives of the sample weighting in the last step must be achieved. Consequently, the proportion of each sub-dataset was checked, and two-sample KS tests were conducted for each parameter in each sub-dataset to compare the marginal distributions in the weighted synthetic crash dataset with their corresponding reference distributions.

Secondly, for each sub-dataset containing multiple parameters, we needed to verify the similarity of the overall multivariate distributions between the synthetic and reference datasets. To do this, we utilized the t-distributed stochastic neighbor embedding (t-SNE) technique [37] to transform the multidimensional data into unidimensional data and then conducted a two-sample KS test on the transformed data.

Lastly, the crash severity levels between the synthetic and reference datasets also needed to be compared. For each synthetic crash, the Delta- v of the lead vehicle (Δv_l) was computed using the Kudlich-Slibar rigid body impulse model [38],

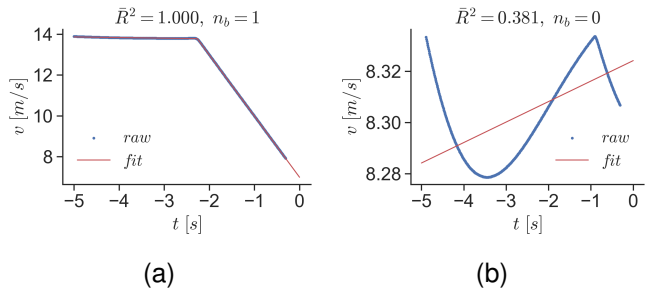


Fig. 5. Examples of speed profile fit results. n_b is the number of breakpoints.

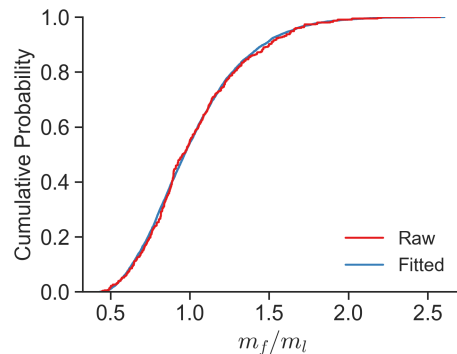


Fig. 6. Fitting of the mass ratio distribution in CISS_m. KS test results: sample size $n = 748$, statistic = 0.04, p-value = 0.79.

in which the coefficient of restitution e (the ratio of the post-impact vehicle-velocity-difference to the pre-impact vehicle-velocity-difference between the two vehicles) was computed as suggested in an existing study [39]:

$$e = 0.47477 - 0.26139 \cdot \log(\Delta v_{pre}) \dots + 0.03382 \cdot (\log(\Delta v_{pre}))^2 \dots - 0.1139 \cdot (\log(\Delta v_{pre}))^3, \quad (5)$$

where Δv_{pre} is the pre-impact vehicle-velocity-difference (m/s). The weighted distribution of Δv_l was then compared with the reference distribution of Δv_l (obtained in REF_1), using the weighted two-sample KS test.

IV. RESULTS

A. Data Combination

1) *Fitting of speed profiles:* The speed profiles of both vehicles in SHRP2_b and PCM_b were fitted into the piecewise linear model. 84.2% (1540 out of 1828) of the speed profiles have an adjusted R-squared \bar{R}^2 greater than 0.9: see Fig. 5(a). Of the remaining 15.8% (288), 93.1% (268) showed a speed change (i.e., the difference between the maximum and minimum speed) of less than 0.5 m/s. For those 268 profiles with only minor speed changes, the piecewise linear model simplified the speed profile as a straight line, which led to a lower \bar{R}^2 : see Fig. 5(b). The remaining 6.9% (20) of the cases have an adjusted R-squared \bar{R}^2 greater than 0.75.

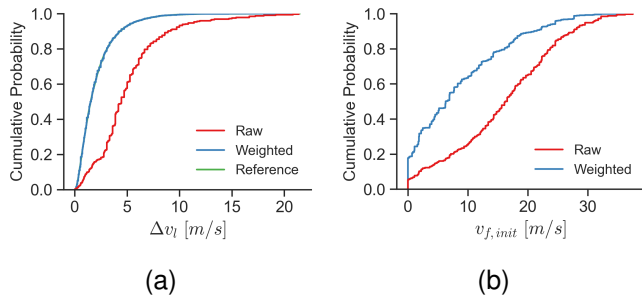


Fig. 7. KNN sample weighting results of the raw dataset COM_f according to the reference distribution of Δv_l : (a) Δv_l , and (b) $v_{f,init}$. The blue and green lines are almost identical in (a). The weighted two-sample KS test results between the weighted samples and reference distribution of Δv_l : valid sample size (i.e., the sum of weights) of the weighted distribution $n = 324$, sample size of the reference distribution $n_r = 10,000$, statistic = 0.03, and p-value = 1.00.

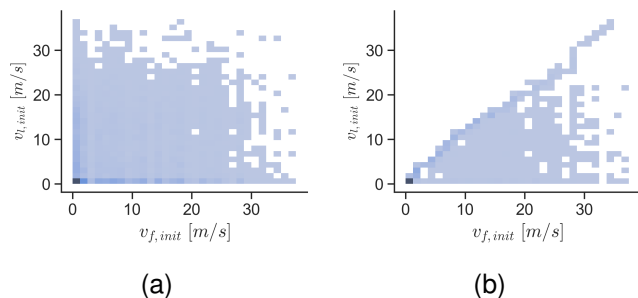


Fig. 8. Joint distribution of $v_{f,init}$ and $v_{l,init}$ before (a) and after (b) pairing samples from $\Phi(v_{l,init}, a_{l,min})$ and $\Phi(v_{f,init}, \Delta v_l)$.

2) *Mass ratio distribution*: The generalized gamma distribution was selected for fitting the mass ratio data in CISS_m. A two-sample KS test was conducted between the raw and the fitted distributions. The results do not indicate any significant difference (see Fig. 6).

3) *Reference datasets*: The samples in the raw dataset COM_f ($n=524$) were weighted using the KNN sample weighting method according to $\tilde{\Phi}(\Delta v_l)$ from REF_1. There were 324 samples with a weight value larger than zero. The cumulative distribution functions (CDFs) of Δv_l and $v_{f,init}$ are shown in Figs. 7 (a)-(b), respectively. The weighted $v_{f,init}$ distribution was then used as the reference distribution of $v_{f,init}$. The weighted two-sample KS test between the weighted samples and the reference distribution of Δv_l shows no significant difference. Compared with the raw distribution, the weighted distribution $\tilde{\Phi}(\Delta v_l, v_{f,init})$ has a higher proportion of low-severity (i.e., small Δv_l) and low-speed (i.e., small $v_{f,init}$) crashes.

The reference dataset REF_i was created by pairing an equal number of samples randomly selected (with replacement) from two reference datasets using the pairing algorithm described in Appendix B. Fig. 8 shows the joint distribution of the initial speeds of both vehicles before and after pairing the selected samples. The target correlations to preserve were: $\tilde{r}(v_{f,init}, v_{l,init}) = 0.78$ and $\tilde{r}(v_{f,init}, a_{l,min}) = -0.54$. The pairing algorithm effectively retained the correlations among relevant

TABLE III
COMPARISON BETWEEN THE WEIGHTED AND REFERENCE MARGINAL DISTRIBUTIONS FOR FOUR WEIGHTING PARAMETERS

Parameter	n^*	n_r^{**}	KS statistic	p-value
$v_{f,init}$	852	10,000	0.08	0.54
Δv_l			0.10	0.32
$v_{l,init}$			0.10	0.29
$a_{l,min}$			0.09	0.43

* Valid sample size = sum of sample weights.

** Sample size of the reference data.

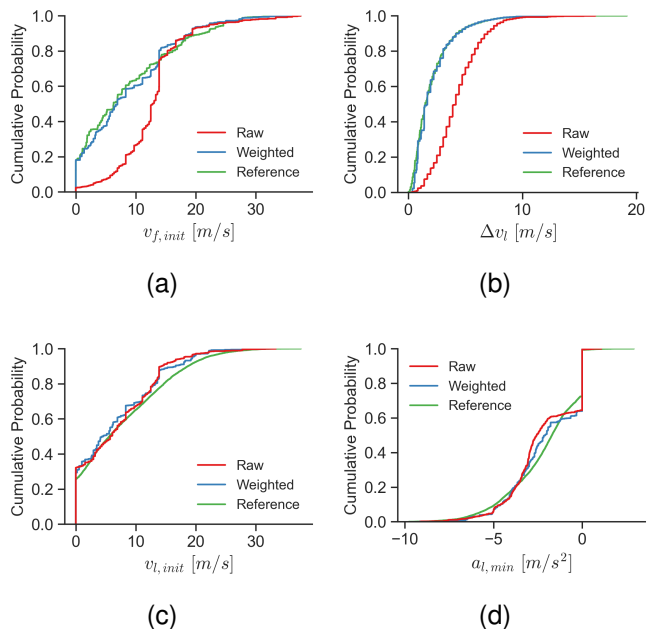


Fig. 9. KNN sample weighting results of the raw combined dataset COM_b (obtained by combining SHRP2_b and COM_b) according to REF_i.

parameters in the pairing results (i.e., REF_i): $r(v_{f,init}, v_{l,init}) = 0.78$ and $r(v_{f,init}, a_{l,min}) = -0.54$.

REF_b (i.e., the reference dataset of the initial states and minimum fitted accelerations of both vehicles) was created by weighting samples in COM_b (the combined dataset of both vehicles) using the KNN sample weighting method according to the intermediate reference dataset REF_i. There were 852 samples (out of 913) with a weight value larger than zero. The weighted two-sample KS tests were conducted to test whether the weighted and the reference data are from the same distribution. The results in Table III do not indicate any significant difference. However, it is worth noting that the lack of significance does not necessarily imply that the datasets are from the same distribution. Nonetheless, a visual comparison of the well-aligned weighted CDFs for each of the four parameters ($v_{f,init}$, Δv_l , $v_{l,init}$, and $a_{l,min}$) in the weighted and reference distributions indicates substantial similarities (see Fig. 9).

B. Modeling of REF_b

1) *Data categorization*: REF_b, the reference dataset of the initial speeds and minimum fitted accelerations of both vehicles and the initial distance, was divided into six sub-

TABLE IV
SIX SUB-DATASETS

Sub-dataset	Conditions		Proportion
	Initial speeds [m/s]	Acceleration* [m/s ²]	
S1	$v_{init,f} > v_{init,l} > 0$	$a_{f,min} \geq 0$	9.6%
S2	$v_{init,f} > v_{init,l} > 0$	$a_{f,min} < 0$	30.9%
S3	$v_{init,f} > v_{init,l} = 0$	—	13.1%
S4	$v_{init,f} = v_{init,l} = 0$	—	16.3%
S5	$0 < v_{init,f} \leq v_{init,l}$	$a_{f,min} \geq 0$	12.6%
S6	$0 < v_{init,f} \leq v_{init,l}$	$a_{f,min} < 0$	17.5%

* $a_{f,min} \geq 0$ m/s² means the following vehicle did not brake in the event, while $a_{f,min} < 0$ m/s² indicates the following vehicle braked in the event.

datasets (based on the relationship between the initial speeds of both vehicles, whether the following vehicle braked, and whether either vehicle was initially stationary).

Table IV shows the six sub-datasets (S1–S6), including their corresponding proportions.

In both S1 and S2, the following vehicle initially approached the moving lead vehicle (i.e., $v_{init,f} > v_{init,l} > 0$ m/s). The following vehicle braked in S2 (i.e., $a_{f,min} < 0$ m/s²), but not in S1 (i.e., $a_{f,min} \leq 0$ m/s²).

In S3, the following vehicle initially approached the stationary lead vehicle – while in S4, both vehicles were initially stationary. Abnormal acceleration behaviors are present in 56.2% of the cases in S4 (9.2% of all cases).

In S5 and S6, the lead vehicle initially moved away from the moving following vehicle. In S6, the following vehicle braked (i.e., $a_{f,min} < 0$ m/s²), while in S5 it did not (i.e., $a_{f,min} \leq 0$ m/s²).

It is important to note that some of the five parameters in certain sub-datasets can be constant. For instance, the following vehicle’s minimum fitted acceleration ($a_{f,min}$) is zero for all cases in S1 since the following vehicle did not brake. Only the non-constant parameters in each sub-dataset were modeled.

2) *Comparison between the synthetic and reference datasets of selected parameters:* A mixture distribution model was constructed for REF_b by combining all distribution models built for each sub-dataset according to sub-dataset proportions. The model was used to create a synthetic dataset containing 10,000 samples of initial states and minimum fitted accelerations of both vehicles (REF_sb). Table V compares the five parameters for the synthetic and reference datasets (REF_sb and REF_b). Although there are minor differences in the weighted mean and standard deviation (SD) of each parameter between the reference and synthetic datasets, the two datasets underwent a weighted two-sample KS test to test if there are significant differences in each of the five parameters. The p-values in Table V indicate no significant differences between the compared datasets. Additionally, Fig. 10 shows that the weighted CDFs for each of the five parameters in the two datasets are well aligned, demonstrating substantial similarities between the two datasets.

C. Simulation

We ran the matching algorithm for the two reference datasets (REF_sl and REF_sb) and selected 5,000 valid simu-

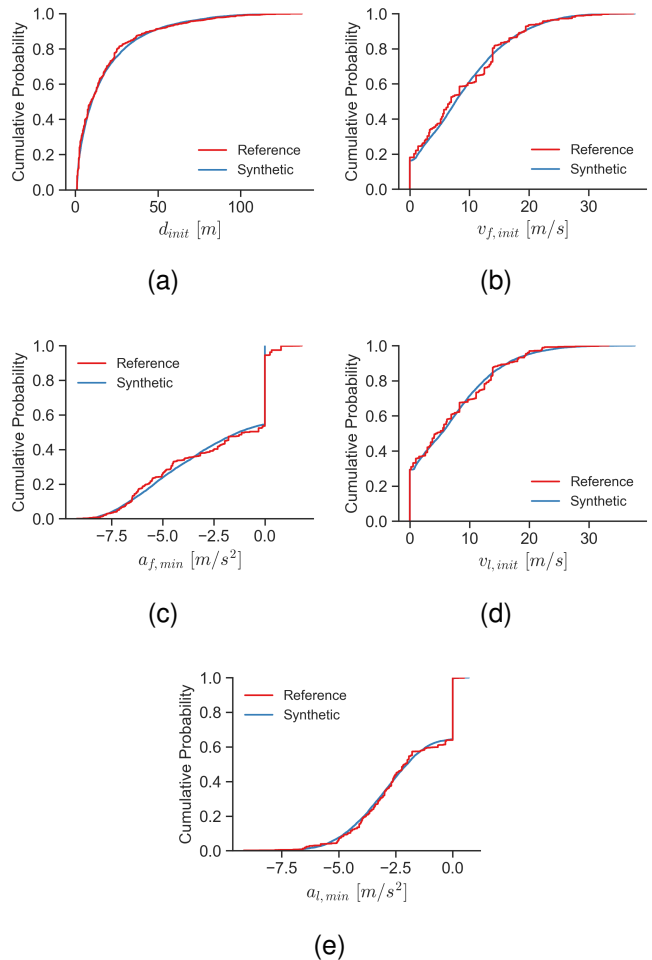


Fig. 10. Weighted CDFs for each of the five parameters in the reference and synthetic datasets: (a) d_{init} , (b) $v_{f,init}$, (c) $a_{f,min}$, (d) $v_{l,init}$, and (e) $a_{l,min}$.

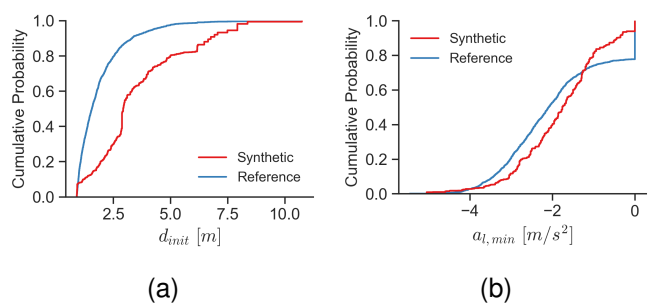


Fig. 11. CDFs of two parameters for the weighted synthetic crash dataset and the corresponding reference distributions: (a) d_{init} in REF_b sub-dataset 4, and (b) $a_{l,min}$ in REF_b sub-dataset 5.

lations to create a synthetic rear-end crash dataset. The sample weighting method outlined in Section III-E3 was used to assign a weight for each sample in the synthetic crash dataset.

Table VI shows the results of the weighted two-sample KS tests between the synthetic crash dataset and the reference datasets (REF_sl, REF_sb, and the reference marginal distributions of the remaining three parameters T , t_g and t_a). There were, in total, 61 tests. At a significance level of

TABLE V
COMPARISON BETWEEN THE SYNTHETIC AND REFERENCE DATASETS OF SELECTED PARAMETERS

Parameter	Unit	Reference ($n = 852^*$)		Synthetic ($n = 10,000$)		KS statistic	p-value
		Mean	SD	Mean	SD		
d_{init}	m	17.62	21.83	18.05	21.10	0.05	0.95
$v_{f,init}$	m/s	8.56	7.49	8.77	7.31	0.07	0.78
$a_{f,min}$	m/s^2	-2.40	2.83	-2.43	2.72	0.06	0.93
$v_{l,init}$	m/s	6.58	6.75	6.68	6.82	0.05	0.94
$a_{l,min}$	m/s^2	-2.03	1.93	-2.06	1.92	0.04	0.99

* Valid sample size = sum of sample weights.

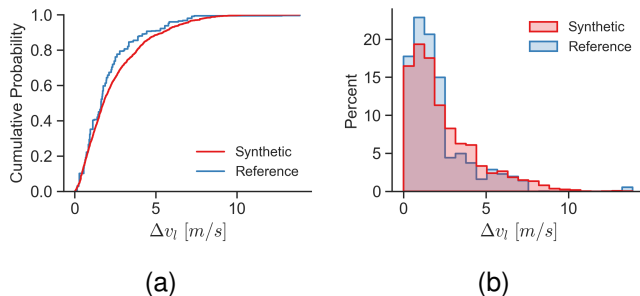


Fig. 12. Comparison between the synthetic crash dataset and the reference dataset for Δv_l : a) CDFs, and b) histograms. The weighted two-sample KS test results between the distributions of Δv_l in the synthetic and reference datasets: sample size of the synthetic dataset $n = 5,000$; sample size of the reference dataset $n_r = 130$; statistic = 0.12, p-value = 0.27.

0.05, approximately three ($\approx 61 \times 0.05$) tests are likely to be incorrectly tested to be significant when they should not be. In our situation, two (less than three) tests show a significant difference at the 0.05 significance level. We looked into those two tests (i.e., the marginal distribution test for d_{init} in REF_b S4 and the marginal distribution test for $a_{l,min}$ in REF_b S5) and analyzed the possible cause.

Fig. 11 shows that the CDFs for the two tests have significant differences. Specifically, Fig. 11(a) shows that fewer valid simulations have a small initial distance (d_{init}), and Fig. 11(b) shows that there are fewer valid simulations in which the lead vehicle did not brake at all during the event (i.e., in which the minimum acceleration $a_{l,min} = 0$ m/s²). These differences can be explained by a limitation in the following vehicle’s acceleration model, the modified IDM; it cannot imitate accelerations as aggressive as those in the real world. For instance, in the cases in Fig. 11(a), the following vehicle was stationary and would not start to move forward unless the distance to the lead vehicle was large enough. (See Section V-B for more discussion.)

Fig. 12 compares the weighted synthetic crash and reference datasets for Δv_l . The results of the weighted two-sample KS test indicate that there is no significant difference between the two datasets. Although the CDFs in Fig. 12(a) are substantially similar, the histograms in Fig. 12(b) illustrate a higher proportion of low values in the reference distribution of Δv_l . This discrepancy could be due to the way that Δv_l was estimated for SHRP2 crashes (in REF_1). During the impact in a rear-end crash, the lead vehicle has a rapid speed increase followed by a swift speed decrease. For these SHRP2 crashes, Δv_l was

calculated as the difference between the post- and pre-impact lead-vehicle speed. The frequency of the lead-vehicle speed signal was 10 Hz; at such a low frequency, the speed signal is unlikely to accurately capture the true post-impact (peak) speed, thereby resulting in an underestimation of Δv_l .

V. DISCUSSION AND CONCLUSIONS

Unlike other studies focusing mainly on injury-involved or policed-reported rear-end crashes [11], [19], [20], this study created a representative synthetic rear-end crash dataset encompassing the full severity range, from physical contact to high-severity levels.

The process of generating synthetic rear-end crash scenarios consists of three main steps: 1) parameterizing the rear-end crashes through modeling the following and lead vehicles, 2) building reference datasets from the parameterized crash data, and 3) generating representative synthetic crash scenarios.

In the first step, a following-vehicle behavior model was developed by combining two existing driver models. The model also included the potential for generating ‘abnormal’ driver acceleration behavior, a phenomenon observed in 9.2% of all crashes. Using this model and the lead-vehicle kinematics model (created in a previous study [21]), we sought to emulate vehicle behaviors that are as similar as possible to those in real-world rear-end crash scenarios. Combining the two vehicle models and the initial states of rear-end crash scenarios created a twelve-dimensional vector representing a rear-end crash.

In the second step, parameterized crash data from multiple crash datasets were combined and weighted to create a reference dataset of the initial states (and minimum fitted accelerations of both vehicles) (REF_b). A synthetic dataset containing these data (REF_sb) was then created by sampling from the distribution model built for REF_b.

At last, simulations were conducted using the following-vehicle behavior model and the two synthetic datasets, REF_sb and REF_sl (a representative synthetic rear-end crash lead-vehicle speed profile dataset created in a previous study [21]). valid simulations were gathered and weighted using an IPF-based weighting algorithm to create a representative synthetic rear-end crash dataset.

In terms of validation, a more comprehensive validation process than in other studies was conducted. Non-parametric statistic tests were implemented for the marginal distributions—not only for the crash outcomes (e.g., Delta-v of the lead vehicle) but also for each of the twelve parameters.

TABLE VI
COMPARISON BETWEEN THE SYNTHETIC CRASH DATASET AND REFERENCE DISTRIBUTIONS

Parameter group	Sub-dataset	Proportion		Parameter	KS statistic	p-value
		Reference	Synthetic			
Initial states and two minimum accelerations	1	0.096	0.092 (-0.004)	d_{init}	0.07	0.91
				$v_{f,init}$	0.10	0.55
				$v_{l,init}$	0.09	0.66
				$a_{l,min}$	0.12	0.30
				Overall	0.12	0.29
	2	0.309	0.291 (-0.018)	d_{init}	0.04	0.67
				$v_{f,init}$	0.06	0.22
				$a_{f,min}$	0.03	0.91
				$v_{l,init}$	0.05	0.47
				$a_{l,min}$	0.03	0.82
	Overall	0.07	0.08			
	3	0.131	0.139 (+0.008)	d_{init}	0.07	0.47
				$v_{f,init}$	0.04	1.00
				$a_{f,min}$	0.05	0.90
				Overall	0.08	0.37
	4	0.163	0.163 (+0.000)	d_{init}	0.50	0.00*
	5	0.126	0.134 (+0.008)	d_{init}	0.07	0.59
				$v_{f,init}$	0.09	0.25
				$v_{l,init}$	0.08	0.37
				$a_{l,min}$	0.16	0.00*
	Overall	0.10	0.11			
	6	0.175	0.182 (+0.007)	d_{init}	0.09	0.10
				$v_{f,init}$	0.08	0.12
				$a_{f,min}$	0.04	0.95
$v_{l,init}$				0.07	0.25	
$a_{l,min}$	0.08	0.14				
Overall	0.08	0.14				
Lead-vehicle speed profile	1	0.255	0.301 (+0.046)	—	—	—
	2	0.105	0.090 (-0.015)	$v_{l,init}$	0.11	0.31
				a_1	0.12	0.17
				Overall	0.13	0.13
	3	0.102	0.080 (-0.022)	$v_{l,init}$	0.05	0.97
				a_1	0.07	0.64
				τ_s	0.05	0.98
				Overall	0.05	0.93
	4	0.157	0.146 (-0.011)	$v_{l,init}$	0.08	0.13
				a_1	0.03	0.98
				a_2	0.07	0.34
				τ_s	0.04	0.95
				τ_1	0.07	0.37
				τ_2	0.04	0.95
	Overall	0.08	0.13			
	5	0.046	0.048 (+0.002)	$v_{l,init}$	0.07	0.98
				a_1	0.17	0.12
				a_2	0.16	0.16
				τ_1	0.15	0.27
	Overall	0.09	0.80			
	6	0.133	0.134 (+0.001)	$v_{l,init}$	0.08	0.23
				a_1	0.04	0.87
				a_2	0.04	0.93
				τ_1	0.03	0.98
Overall	0.08	0.20				
7	0.202	0.201 (-0.001)	$v_{l,init}$	0.09	0.11	
			a_1	0.10	0.07	
			a_2	0.05	0.83	
			τ_s	0.10	0.10	
			τ_1	0.04	0.95	
			τ_2	0.07	0.35	
Overall	0.10	0.07				
The remaining three parameters	—	—	T	0.05	0.86	
			t_g	0.05	0.75	
			t_a	0.07	0.82	

* The difference is significant at the 0.05 significance level.

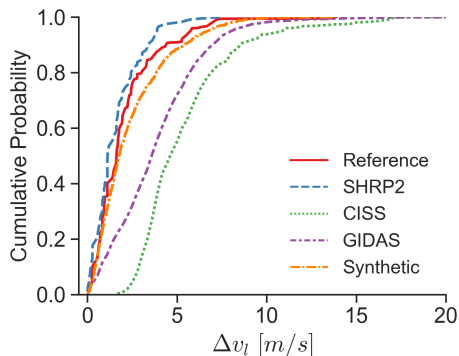


Fig. 13. CDF curves for Δv_l in rear-end crashes among various datasets.

A. Contributions

This study created a representative dataset of synthetic rear-end crashes covering the full range of severity levels. This dataset can be used for safety assessments of ADAS and ADS and as a benchmark when evaluating the representativeness of scenarios generated through other methods (such as traffic-simulation-based and machine-learning-based). Fig. 13 compares the CDF curves of the lead vehicle’s Delta- v in rear-end crashes from various datasets. Compared to the reference dataset, the CISS and GIDAS datasets are biased towards severe crashes. Although the SHRP2 dataset is similar to the reference dataset, it lacks high-severity cases (the maximum Δv_l in the SHRP2 dataset is 7.4 m/s). In contrast, the synthetic crash dataset, mirroring the reference dataset, encompasses crashes with Δv_l reaching 13.8 m/s. As mentioned in Section IV-C, the synthetic dataset exhibits a strong resemblance to the reference dataset regarding the distribution of Delta- v of the lead vehicle.

The methodological contributions of this study mainly lie in the data combination (including sample weighting) methods. In the study, none of the available crash datasets contain all necessary signals without substantial bias; this shortcoming is common in data-driven studies. We used a set of methods to combine and weight data from multiple crash datasets to mitigate the biases. Among these methods, the KNN sample weighting method is particularly noteworthy because, unlike conventional post-stratification methods, it can be used to weight biased data to match a reference dataset even when omitted strata exist. In the future, these data combination methods can be applied when creating a multivariate joint distribution is needed and the only datasets available contain biased data or incomplete signals.

B. Limitations and future work

Our previous study [21] relied on pre-crash data from the United States to establish the reference dataset of lead-vehicle kinematics. However, we faced a shortage of crash data involving both vehicles: SHRP2_b contained only 37 samples. Therefore, we had to use the available data from the GIDAS-PCM dataset (PCM_b), even though it was from Germany. We assumed that rear-end crashes in the US and Germany

have similar mechanisms, although their distributions may differ. Moreover, during data combination, the KNN sample weighting method was applied to reduce bias in the merged raw data (SHRP2_b and PCM_b) so that the weighted data could match the reference dataset created using the US crash data. In addition, in Sub-step 4 of the data combination step, we used the optimal pairing results of samples from the two reference datasets REF_l and REF_f as an approximation for the reference dataset of the four parameters ($v_{f,init}$). This compromise was necessary because no such reference dataset is available (at least not to us).

The modified IDM was used to simulate the acceleration behavior of the following vehicle. However, the model was designed and calibrated to replicate naturalistic car-following behaviors rather than crashes. As a result, this model cannot accurately mimic highly aggressive accelerations, which often occur in real-world situations. Thus, as mentioned in Section IV-C, a subset of crash scenarios in REF_b sub-datasets S4-5 was missing. To address this limitation, future research should try calibrating the modified IDM acceleration model using pre-crash data for scenario generation.

As mentioned in Section IV-C, the low-frequency speed signal used to estimate the Delta- v of the lead vehicle in the SHRP2 dataset might underestimate the true value. Future research should either find a better estimation method or use data with a higher frequency.

ACKNOWLEDGMENTS

This research was funded by FFI Vinnova, a Swedish governmental agency for innovation, as part of the project Improved quantitative driver behavior models and safety assessment methods for ADAS and AD (QUADRIS: nr. 2020-05156). The SHRP2 data used in this study has the identifier DOI SHRP2-DUL-16-172 and was made available to us by the Virginia Tech Transportation Institute (VTTI) under a Data License Agreement. The findings and conclusions of this paper are those of the authors and do not necessarily represent the views of VTTI, the Transportation Research Board (TRB), or the National Academies. The authors wish to thank Mikael Ljung Aust at Volvo Cars Safety Centre for reviewing the manuscript.

APPENDIX A

KNN SAMPLE WEIGHTING ALGORITHM

Since raw distributions from datasets can often be biased with respect to one or more parameters, the sample weighting process aims to assign weights to samples in raw distributions $\{\mathbf{X}_i | i \in [1, n]\}$ (where $\mathbf{X}_i = [x_1^{(i)}, \dots, x_K^{(i)}]^T$) so that the weighted data matches the known reference distribution of a subset of parameters $\hat{\Phi}(x_1, \dots, x_m)$ ($m < K$).

Post-stratification weighting [40] is one possibility. It is a statistical technique commonly used in survey research to reduce bias and improve the accuracy of population estimates. It involves dividing the target population into strata based on certain characteristics or variables, collecting data within each stratum, and then assigning weights to the observations based on the target population distribution within each stratum.

Typically, binning is used to create strata when the variables are continuous. The weight for observations in each stratum is the target population total divided by the number of observations in the stratum. In our situation, the raw samples (i.e., observations) $\{\mathbf{X}_i | i \in [1, n]\}$ should be grouped into discrete bins designed based on the known reference distribution (i.e., target population) $\tilde{\Phi}(x_1, \dots, x_m)$. However, this method assumes that no strata are omitted. In other words, observations within all bins must correspond to the reference distribution. In our case, omitted strata did exist in the combined data. One possible cause could be the bias in the combined data. For instance, datasets sourced from CISS and GIDAS-PCM contain only severe crashes. Therefore, a novel method, the k-nearest neighbors (KNN) sample weighting method, was proposed to handle this issue.

The KNN sample weighting method can be seen as a post-stratification weighting method with a dynamic binning strategy. Each sample extracted from the known reference distribution carries a weight of one. For each extracted sample, the k-nearest raw samples are grouped into one bin to share the weight (see Step 3c in the following algorithm). It is also worth mentioning that samples that have never been selected as the nearest neighbors of any extracted sample will have a weight of zero.

Algorithm 1 KNN sample weighting algorithm.

Set $w_i = 0 \forall i \in [1, n]$
 Generate N samples from $\tilde{\Phi}(x_1, \dots, x_m)$:
 $\{\tilde{x}_1^{(j)}, \dots, \tilde{x}_m^{(j)}\}^T | j \in [1, N]\}$
 For $j = 1$ to N :
 $d_j^{(i)} = \sqrt{\sum_{p=1}^m (\tilde{x}_p^{(j)} - x_p^{(i)})^2} \forall i \in [1, n]$
 $\omega_j^{(i)} = 1/d_j^{(i)}$ if all $(d_j^{(i)} > 0)$ else $I_{\{d_j^{(i)} = 0\}} \forall i \in [1, n]$
 $H = \arg \max_i (\{\omega_j^{(i)} | i \in [1, n]\}, k)$
 $w_{h_l} \leftarrow w_{h_l} + \frac{\omega_j^{(h_l)}}{\sum_{i=1}^k \omega_j^{(h_l)}} \forall h_l \in H$
 $w_i \leftarrow \frac{w_i}{\sum_{i=1}^n w_i} \sum_{i=1}^n I_{\{w_i > 0\}} \forall i \in [1, n]$

As shown in Algorithm 1, the KNN sample weighting method contains four main steps.

- 1) Set the initial sample weight for each raw sample to zero: $w_i = 0 \forall i \in [1, n]$.
- 2) Sample N samples from the known reference distribution $\tilde{\Phi}(x_1, \dots, x_m)$.
- 3) For any generated sample $\tilde{\mathbf{X}}_j$:
 - a) Compute the Euclidean distance between $\tilde{\mathbf{X}}_j$ and \mathbf{X}_i , $d_j^{(i)}$, for all $i \in [1, n]$. ($\tilde{x}_p^{(j)}$ and $x_p^{(i)}$ are the standardized values of $\tilde{x}_p^{(j)}$ and $x_p^{(i)}$, respectively.)
 - b) Compute the distributing weight of the raw sample \mathbf{X}_i for $\tilde{\mathbf{X}}_j$, $\omega_j^{(i)}$, for all $i \in [1, n]$. (A smaller Euclidean distance correlates to a higher distributing weight.)
 - c) Distribute a weight value of one among the top k raw samples with the highest distributing weights ($\{\mathbf{X}_{h_l} | h_l \in H\}$).

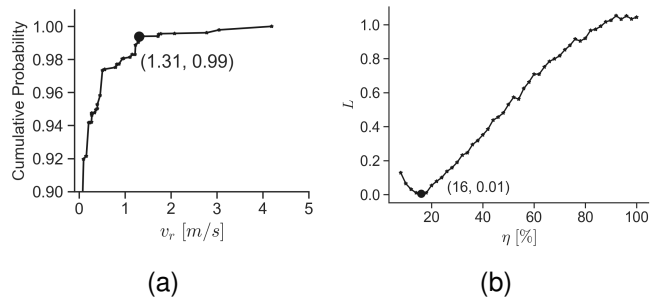


Fig. 14. Pairing algorithm parameter setting: a) CDF of the lead vehicle's initial relative speed ($v_{l,init} - v_{f,init}$), and b) Loss of the pairing as a function of η .

- 4) Scale the weights so that $\sum_{i=1}^n w_i = n$.

The value of k is determined by minimizing the loss, $\sum_{l=1}^m s_l^{(k)}$, where $s_l^{(k)}$ is the KS statistic for x_l conditioned on k computed with the weighted two-sample KS tests between the weighted x_l data and the reference data $\{\tilde{x}_l^{(j)} | j \in [1, N]\}$.

APPENDIX B PAIRING ALGORITHM

The pairing algorithm was mainly based on the relationship between the initial speeds of both vehicles ($v_{f,init}$ and $v_{l,init}$) because these two parameters have a stronger correlation than the one between the following vehicle's initial speed ($v_{f,init}$) and the lead vehicle's minimum fitted acceleration ($a_{l,min}$). We also observed that $v_{l,init}$ is no larger than $v_{f,init}$ in most cases.

As shown in Algorithm 2, η is the percentage of randomly selected samples from set A , $v_{r,thd}$ ($= v_{l,init} - v_{f,init}$) is the threshold of the lead vehicle's initial relative speed (m/s), $f_{v_{l,init}}$ is the probability density function of $v_{l,init}$ (estimated using the marginal distribution of $v_{l,init}$ from REF_1), L is the loss, and η^* is the optimal η with minimum loss. A smaller η leads to a stronger correlation between $v_{f,init}$ and $v_{l,init}$ (as for $v_{f,init}$ and $a_{l,min}$). $v_{r,thd}$ was set to 1.31 m/s, the elbow point in its CDF curve: see Fig. 14(a). η^* was set to 0.16 with a minimum loss of 0.01: see Fig. 14(b).

APPENDIX C MATCHING ALGORITHM

The algorithm is shown in Algorithm 3. n_{iter} is the current number of iterations in terms of lead-speed profile, $n_{iter,max}$ is the maximum number of iterations (set to 10 in this study), $d_j^{(i)}$ is the Euclidean distance between \mathbf{V}_j and \mathbf{U}_i , W is the set of candidates in U that can pair with \mathbf{V}_j . \bar{T} and \bar{T}_g are the sets of percentiles $\{\pi_p | p \in \{0.01, 0.02, \dots, 0.99\}\}$ from their marginal distributions. \bar{T}^* , \bar{t}_g^* , and \bar{t}_a^* are sets containing corresponding parameter candidates. The function `update_candidates_W` updates W according to the sub-dataset that \mathbf{V}_j belongs to. (For instance, a \mathbf{V}_j from S1 requires that $v_{f,init} > v_{l,init} > 0$.) The functions `update_candidates_T`, `update_candidates_t_g` and `update_candidates_t_a` update \bar{T}^* , \bar{t}_g^* and \bar{t}_a^* , respectively. These functions were designed based on the monotonous correlation between the parameter (T , t_g , or

Algorithm 2 Pairing algorithm.

Sample with the replacement of N samples from $\tilde{\Phi}(v_{f,init}, \Delta v_l)$ and $\tilde{\Phi}(v_{l,init}, a_{l,min})$, respectively:
 $A = \{\mathbf{A}_i | i \in [1, N]\}$, $B = \{\mathbf{B}_j | j \in [1, N]\}$, where $\mathbf{A}_i = [\tilde{v}_{f,init}^{(i)}, \tilde{\Delta v_l}^{(i)}]^T$ and $\mathbf{B}_j = [\tilde{v}_{l,init}^{(j)}, \tilde{a}_{l,min}^{(j)}]^T$
For $\eta = 0 : 2 : 100$ [%]:
Select randomly η samples out of A
Create a copy of B : $\hat{B} = B$
For each selected sample \mathbf{A}_i , select its corresponding $\hat{\mathbf{B}}_i$ from \hat{B} :
If $\tilde{v}_{l,init}^{(j)} > \tilde{v}_{f,init}^{(i)} + v_{r,thd} \forall \mathbf{B}_j \in \hat{B}$:
Select the one with the minimum $\tilde{v}_{l,init}$
Else:
Select based on $f_{v_{l,init}}(v_{l,init} | v_{l,init} \leq \tilde{v}_{f,init}^{(i)} + v_{r,thd})$
Drop $\hat{\mathbf{B}}_i$ from \hat{B}
Sort the remaining samples in A in ascending order of $\tilde{v}_{f,init}$: $\{\mathbf{A}_p | p \in P\}$
For each \mathbf{A}_p , select its corresponding $\hat{\mathbf{B}}_p$ from B (same as for \mathbf{A}_i)
Compute correlations for paired samples:
 $r(v_{f,init}, v_{l,init})$, $r(v_{f,init}, a_{l,min})$, $r(\Delta v_l, v_{l,init})$, and $r(\Delta v_l, a_{l,min})$
Compute the loss for paired samples:
If $|r(\Delta v_l, v_{l,init})| < 0.3$ & $|r(\Delta v_l, a_{l,min})| < 0.3$:
 $L(\eta) = |r(v_{f,init}, v_{l,init}) - \tilde{r}(v_{f,init}, v_{l,init})| + |r(v_{f,init}, a_{l,min}) - \tilde{r}(v_{f,init}, a_{l,min})|$
Else:
 $L(\eta) = +\infty$
 $\eta^* = \arg \min_x L(x)$

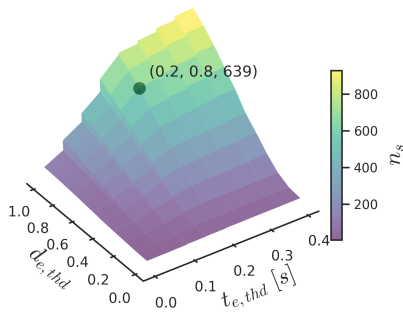


Fig. 15. Selection of $t_{e,thd}$ and $d_{e,thd}$.

t_a) and the crash moment t_c . (For instance, a larger T would result in the vehicle maintaining a longer following distance, delaying any potential crash.) Therefore, if the current t_c is less than five seconds, the T candidates for the next iteration must be larger than the current value of T . The simulation function `sim` is described in Section III-E1.

To determine the two threshold values $t_{e,thd}$ and $d_{e,thd}$, a subset with a sample size of 200 was randomly extracted from REF_sl and REF_sb, respectively (U and V). For each $\mathbf{U}_i \in U$ and each $\mathbf{V}_j \in V$, we looped through \bar{T}^* and \bar{T}_g^* to find the event with the minimum crash moment error t_e . The total number of valid simulations n_s is a function of $t_{e,thd}$ and $d_{e,thd}$ (see Fig. 15). The elbow point in the surface was selected: $d_{e,thd} = 1.0$, $t_{e,thd} = 0.2$ s.

REFERENCES

- [1] A. K. Pradhan, A. Hungund, D. E. Sullivan *et al.*, “Impact of advanced driver assistance systems (adas) on road safety and implications for ed-

- ucation, licensing, registration, and enforcement,” Massachusetts. Dept. of Transportation. Office of Transportation Planning, Tech. Rep., 2022.
- [2] S. Feng, Y. Feng, X. Yan, S. Shen, S. Xu, and H. X. Liu, “Safety assessment of highly automated driving systems in test tracks: A new framework,” *Accident Analysis & Prevention*, vol. 144, p. 105664, 2020.
- [3] R. Donà and B. Ciuffo, “Virtual testing of automated driving systems. a survey on validation methods,” *IEEE Access*, vol. 10, pp. 24 349–24 367, 2022.
- [4] J. Cai, W. Deng, H. Guang, Y. Wang, J. Li, and J. Ding, “A survey on data-driven scenario generation for automated vehicle testing,” *Machines*, vol. 10, no. 11, p. 1101, 2022.
- [5] Z. Szalay, “Critical scenario identification concept: the role of the scenario-in-the-loop approach in future automotive testing,” *IEEE Access*, 2023.
- [6] P. Wimmer, O. Op_Den_Camp, H. Weber, H. Chajmowicz, M. Wagner, J. L. Mallada, F. Fahrenkrog, and F. Denk, “Harmonized approaches for baseline creation in prospective safety performance assessment of driving automation systems,” in *27th International Technical Conference on the Enhanced Safety of Vehicles (ESV), Yokohama, Japan, 2023*, pp. 3–6.
- [7] S. Feng, X. Yan, H. Sun, Y. Feng, and H. X. Liu, “Intelligent driving intelligence test for autonomous vehicles with naturalistic and adversarial environment,” *Nature communications*, vol. 12, no. 1, p. 748, 2021.
- [8] W. Baron, C. Sippl, K.-S. Hielscher, and R. German, “Repeatable simulation for highly automated driving development and testing,” in *2020 IEEE 91st Vehicular Technology Conference (VTC2020-Spring)*. IEEE, 2020, pp. 1–7.
- [9] S. Shah, D. Dey, C. Lovett, and A. Kapoor, “Airsim: High-fidelity visual and physical simulation for autonomous vehicles,” in *Field and Service Robotics: Results of the 11th International Conference*. Springer, 2018, pp. 621–635.
- [10] J. M. Scanlon, K. D. Kusano, T. Daniel, C. Alderson, A. Ogle, and T. Victor, “Waymo simulated driving behavior in reconstructed fatal crashes within an autonomous vehicle operating domain,” *Accident Analysis & Prevention*, vol. 163, p. 106454, 2021.
- [11] M. Bareiss, J. Scanlon, R. Sherony, and H. C. Gabler, “Crash and injury prevention estimates for intersection driver assistance systems in left turn across path/opposite direction crashes in the united states,” *Traffic injury prevention*, vol. 20, no. sup1, pp. S133–S138, 2019.
- [12] H. Hamdane, T. Serre, C. Masson, and R. Anderson, “Issues and challenges for pedestrian active safety systems based on real world accidents,” *Accident Analysis & Prevention*, vol. 82, pp. 53–60, 2015.

Algorithm 3 Matching algorithm.

Sample with the replacement of N samples from REF_sl and REF_sb, respectively:

$$U = \{\mathbf{U}_i \mid i \in [1, N]\}, \text{ where } \mathbf{U}_i = [\tilde{v}_{l,init}^{(i)}, \tilde{a}_{l,min}^{(i)}, \tilde{a}_1^{(i)}, \tilde{a}_2^{(i)}, \tilde{\tau}_s^{(i)}, \tilde{\tau}_1^{(i)}, \tilde{\tau}_2^{(i)}]^T$$

$$V = \{\mathbf{V}_j \mid j \in [1, N]\}, \text{ where } \mathbf{V}_j = [\tilde{d}_{init}^{(j)}, \tilde{v}_{f,init}^{(j)}, \tilde{a}_{f,min}^{(j)}, \tilde{v}_{l,init}^{(*j)}, \tilde{a}_{l,min}^{(*j)}]^T$$

For $j = 1$ to N :

Set default values: $valid = \text{False}$, $log = \text{None}$, $n_{iter} = 0$

$$d_j^{(i)} = \sqrt{(\tilde{v}_{l,init}^{(i)} - \tilde{v}_{l,init}^{(*j)})^2 + (\tilde{a}_{l,min}^{(i)} - \tilde{a}_{l,min}^{(*j)})^2} \quad \forall i \in [1, N]$$

$$W = \{\mathbf{U}_i \mid d_j^{(i)} \leq d_{e,thd}, i \in [1, N]\}$$

$W \leftarrow \text{update_candidates_}W(W)$

While (not $valid$) and ($n(W) > 0$) and ($n_{iter} < n_{iter,max}$):

$n_{iter} \leftarrow n_{iter} + 1$

Create candidates for the three parameters: \bar{T}^* , \bar{t}_g^* , \bar{t}_a^*

Select randomly \mathbf{W}_l from W and drop it from W

While (not $valid$) and ($n(\bar{T}) > 0$):

If log is not None:

$\bar{T}^* \leftarrow \text{update_candidates_}T(log, \bar{T}^*)$

If $n(\bar{T}^*) = 0$: break

Select randomly $T^{(m)}$ from \bar{T}^* and drop it from \bar{T}^*

While (not $valid$) and ($n(\bar{t}_g) > 0$):

If log is not None:

$\bar{t}_g^* \leftarrow \text{update_candidates_}t_g(log, \bar{t}_g^*)$

If $n(\bar{t}_g^*) = 0$: break

Select randomly $t_g^{(h)}$ from \bar{t}_g^* and drop it from \bar{t}_g^*

If abnormal_acceleration(\mathbf{V}_j):

While (not $valid$) and ($n(\bar{t}_a) > 0$):

If log is not None:

$\bar{t}_a^* \leftarrow \text{update_candidates_}t_a(log, \bar{t}_a^*)$

If $n(\bar{t}_a^*) = 0$: break

Select randomly $t_a^{(q)}$ from \bar{t}_a^* and drop it from \bar{t}_a^*

$valid, log = \text{sim}(\mathbf{V}_i, \mathbf{W}_l, T^{(m)}, t_g^{(h)}, t_a^{(q)})$

Else:

$valid, log = \text{sim}(\mathbf{V}_i, \mathbf{W}_l, T^{(m)}, t_g^{(h)}, +\infty)$

If $valid$: Save log

- [13] S. H. Haus and H. C. Gabler, "The potential for active safety mitigation of us vehicle-bicycle crashes," *Future Active Safety Technology Towards Zero Traffic Accidents (FAST-Zero)*, 2019.
- [14] J. Bärghman, C.-N. Boda, and M. Dozza, "Counterfactual simulations applied to shrp2 crashes: The effect of driver behavior models on safety benefit estimations of intelligent safety systems," *Accident Analysis & Prevention*, vol. 102, pp. 165–180, 2017.
- [15] Y. Ma, C. Sun, J. Chen, D. Cao, and L. Xiong, "Verification and validation methods for decision-making and planning of automated vehicles: A review," *IEEE Transactions on Intelligent Vehicles*, vol. 7, no. 3, pp. 480–498, 2022.
- [16] P. Olleja, J. Bärghman, and N. Lubbe, "Can non-crash naturalistic driving data be an alternative to crash data for use in virtual assessment of the safety performance of automated emergency braking systems?" *Journal of safety research*, vol. 83, pp. 139–151, 2022.
- [17] A. Arun, M. M. Haque, A. Bhaskar, S. Washington, and T. Sayed, "A systematic mapping review of surrogate safety assessment using traffic conflict techniques," *Accident Analysis & Prevention*, vol. 153, p. 106016, 2021.
- [18] A. Leledakis, M. Lindman, J. Östh, L. Wågström, J. Davidsson, and L. Jakobsson, "A method for predicting crash configurations using counterfactual simulations and real-world data," *Accident Analysis & Prevention*, vol. 150, p. 105932, 2021.
- [19] A. Gambi, T. Huynh, and G. Fraser, "Generating effective test cases for self-driving cars from police reports," in *Proceedings of the 2019 27th ACM Joint Meeting on European Software Engineering Conference and Symposium on the Foundations of Software Engineering*, 2019, pp. 257–267.
- [20] X. Wang, Y. Peng, T. Xu, Q. Xu, X. Wu, G. Xiang, S. Yi, and H. Wang, "Autonomous driving testing scenario generation based on in-depth vehicle-to-powered two-wheeler crash data in china," *Accident Analysis & Prevention*, vol. 176, p. 106812, 2022.
- [21] J. Wu, C. Flannagan, U. Sander, and J. Bärghman, "Modeling lead-vehicle kinematics for rear-end crash scenario generation," *IEEE Transactions on Intelligent Transportation Systems*, 2024.
- [22] O. Derbel, T. Peter, H. Zebiri, B. Mourllion, and M. Basset, "Modified intelligent driver model for driver safety and traffic stability improvement," *IFAC Proceedings Volumes*, vol. 46, no. 21, pp. 744–749, 2013.
- [23] M. Svärd, G. Markkula, J. Bärghman, and T. Victor, "Computational modeling of driver pre-crash brake response, with and without off-road glances: Parameterization using real-world crashes and near-crashes," *Accident Analysis & Prevention*, vol. 163, p. 106433, 2021.
- [24] F. Zhang, E. Y. Noh, R. Subramanian, and C.-L. Chen, "Crash investigation sampling system: Sample design and weighting," Tech. Rep., 2019.
- [25] R. Subramanian and E. Acevedo-Díaz, "Crash investigation sampling system 2019 data manual," Tech. Rep., 2020.
- [26] J. M. Hankey, M. A. Perez, and J. A. McClafferty, "Description of the shrp 2 naturalistic database and the crash, near-crash, and baseline data sets," Virginia Tech Transportation Institute, Tech. Rep., 2016.
- [27] A. Schubert, H. Liers, and M. Petzold, "The gidas pre-crash-matrix 2016: Innovations for standardized pre-crash-scenarios on the basis of the vufo simulation model vast," 2017.
- [28] T. Victor, M. Dozza, J. Bärghman, C.-N. Boda, J. Engström, C. Flannagan, J. D. Lee, and G. Markkula, "Analysis of naturalistic driving study data: Safer glances, driver inattention, and crash risk," Tech. Rep., 2015.

- [29] M. Svård, G. Markkula, J. Engström, F. Granum, and J. Bårgman, "A quantitative driver model of pre-crash brake onset and control," in *Proceedings of the Human Factors and Ergonomics Society Annual Meeting*, vol. 61, no. 1. SAGE Publications Sage CA: Los Angeles, CA, 2017, pp. 339–343.
- [30] D. N. Lee, "A theory of visual control of braking based on information about time-to-collision," *Perception*, vol. 5, no. 4, pp. 437–459, 1976.
- [31] J. Bårgman, V. Lisovskaja, T. Victor, C. Flannagan, and M. Dozza, "How does glance behavior influence crash and injury risk? a 'what-if' counterfactual simulation using crashes and near-crashes from shrp2," *Transportation Research Part F: Traffic Psychology and Behaviour*, vol. 35, pp. 152–169, 2015.
- [32] G. Markkula, J. Engström, J. Lodin, J. Bårgman, and T. Victor, "A farewell to brake reaction times? kinematics-dependent brake response in naturalistic rear-end emergencies," *Accident Analysis & Prevention*, vol. 95, pp. 209–226, 2016.
- [33] I. Cohen, Y. Huang, J. Chen, J. Benesty, J. Benesty, J. Chen, Y. Huang, and I. Cohen, "Pearson correlation coefficient," *Noise reduction in speech processing*, pp. 1–4, 2009.
- [34] J. Pasek, A. Tahk, G. Culter, and M. Schwemmler, *weights: Weighting and Weighted Statistics*, 2021, r package version 1.0.4. [Online]. Available: <https://CRAN.R-project.org/package=weights>
- [35] A.-A. Choupani and A. R. Mamdoohi, "Population synthesis using iterative proportional fitting (ipf): A review and future research," *Transportation Research Procedia*, vol. 17, pp. 223–233, 2016.
- [36] H. Roux de Bezieux, *Ecume: Equality of 2 (or k) Continuous Univariate and Multivariate Distributions*, 2021, r package version 0.9.1. [Online]. Available: <https://CRAN.R-project.org/package=Ecume>
- [37] L. Van der Maaten and G. Hinton, "Visualizing data using t-sne." *Journal of machine learning research*, vol. 9, no. 11, 2008.
- [38] H. Kudlich, *Beitrag zur Mechanik des Kraftfahrzeug-Verkehrsunfalls*, na, 1966.
- [39] J. Leifer, "A supplemental analysis of selected two-vehicle front-to-rear collisions from the nass/cds," *Society of Automotive Engineering (SAE)*, 2013.
- [40] D. Holt and T. F. Smith, "Post stratification," *Journal of the Royal Statistical Society Series A: Statistics in Society*, vol. 142, no. 1, pp. 33–46, 1979.



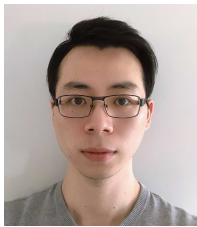
Volvo Cars, leading the analysis of field data with a focus on crashes and their consequences.

Ulrich Scander received his B.S. degree in Biomedical Engineering from the University of Aachen, Germany, in 1997 and his M.S. degree in Accident Research from Graz University of Technology, Austria, in 2008. He received his Ph.D. in Machine and Vehicle Systems from Chalmers University of Technology, Gothenburg, Sweden. He has worked for over 20 years in different positions, such as data analyst and senior principal researcher at Autoliv Research in Germany and Sweden. Since 2022, he has been a Technical Expert at the Safety Centre of



Safety. He received his Ph.D. in Machine and Vehicle Systems from the same university in 2016 and is currently a Professor. He is also the examiner for the course "Vehicle and Traffic Safety" in the master's degree program in Mobility Engineering. His main research interests are virtual safety assessment and its components, including driver behavior modeling, scenario generation, and statistical methods.

Jonas Bårgman received his M.Sc. degree in Mechanical Engineering at Chalmers University of Technology, Gothenburg, Sweden in 1997. After his degree, he worked as an industry researcher in in-crash safety at Autoliv Research for three years and as a software developer at AB Volvo for two years. At this point, he continued his career at Autoliv Research (again) in the domain of pre-crash safety, focusing on human factors and driver behavior. In 2009, he started working at Chalmers University of Technology to build a research group on Active



Jian Wu received his B.S. and M.S. degrees in automotive engineering from Tsinghua University, Beijing, China, in 2013 and 2016. He is now an industrial Ph.D. candidate with Volvo Cars Safety Center and the Department of Mechanics and Maritime Sciences, Chalmers University of Technology, Göteborg, Sweden. He is the author or coauthor of four journal papers and two conference papers. His current research interests include driver behavior modeling, crash data synthesis, and the safety assessments of vehicle safety technologies.



Carol Flannagan received an M.A. in Statistics and a Ph.D. in Mathematical Psychology from the University of Michigan. She is a Research Professor at the University of Michigan Transportation Research Institute (UMTRI) in Ann Arbor, Michigan, USA, and an Affiliated Associate Professor at Chalmers University, Göteborg, Sweden. Her work in transportation research encompasses the analysis of a wide variety of transportation-related data and the development of innovative statistical methods for transportation research. She is currently working on

a number of projects related to safety assessment and benefits assessment for advanced technologies, including ADS.